

## 4. Measurement of Ionization

### 4.1 Gaseous Ionization Detectors

- Ionization chamber
- Ionization yield, charge multiplication
- Proportional counter
- Geiger-Müller counter
- Streamer tubes

### 4.2 Ionization in liquids

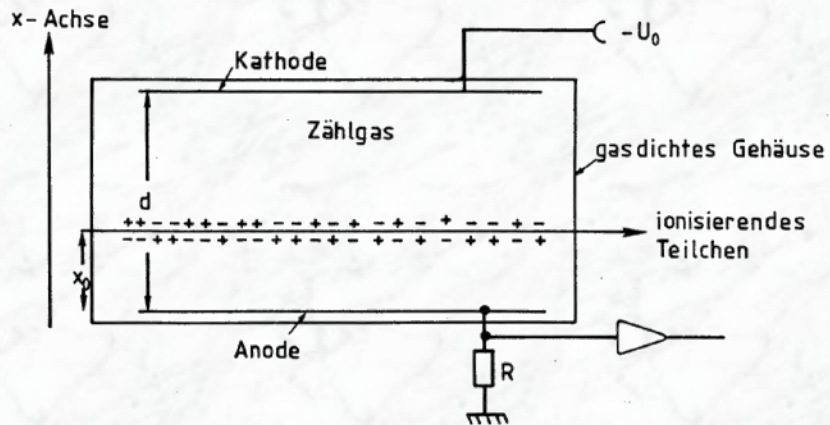
### 4.3 Drift and diffusion in gases

# History of Instrumentation

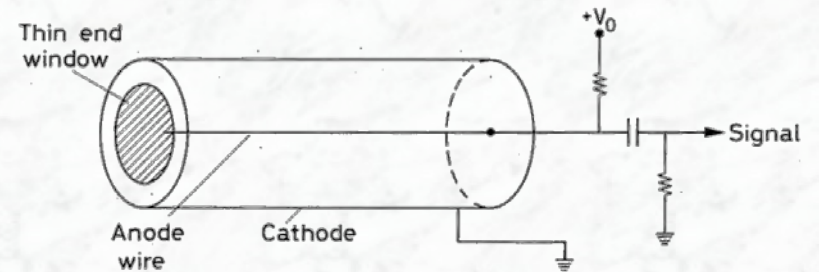
1906:	Geiger Counter	H. Geiger, E. Rutherford
1910:	Cloud Chamber	C.T.R. Wilson
1928:	Geiger-Müller Counter*	W. Müller
1929:	Coincidence Method	W. Bothe
1930:	Emulsion	M. Blau
1940/50:	Scintillator, Photomultiplier*	
1952:	Bubble Chamber	D. Glaser
1962:	Spark Chamber	
1968:	Multi-Wire Prop. Chamber*	G. Charpak
1972:	Drift Chamber*	F. Sauli, J. Heintze et al.
1974:	Time Projection Chamber*	D. Nygren
1983:	Silicon strip detectors*	J. Kemmer, R. Klanner, G. Lutz et al.
1990:	Silicon pixel detectors*	

....

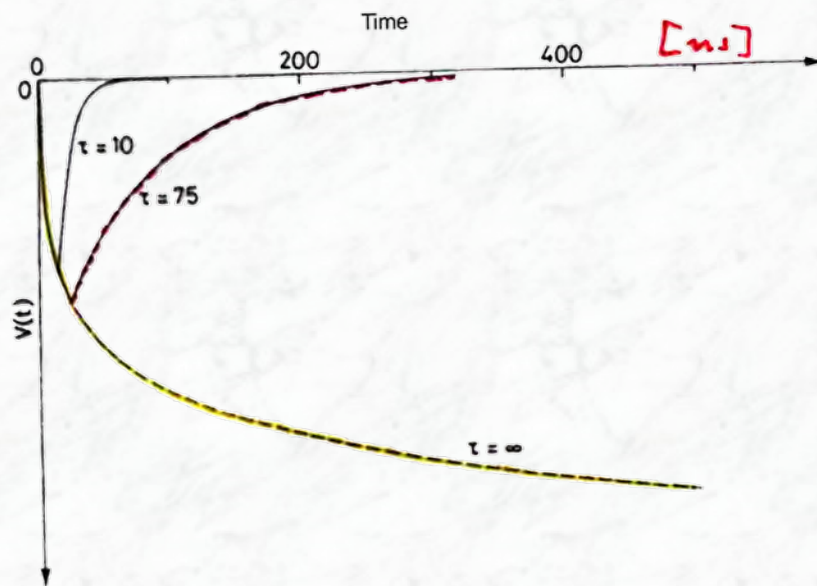
\*covered during this lecture series



Principle of a planar ionization chamber  
[from Ref. 3]

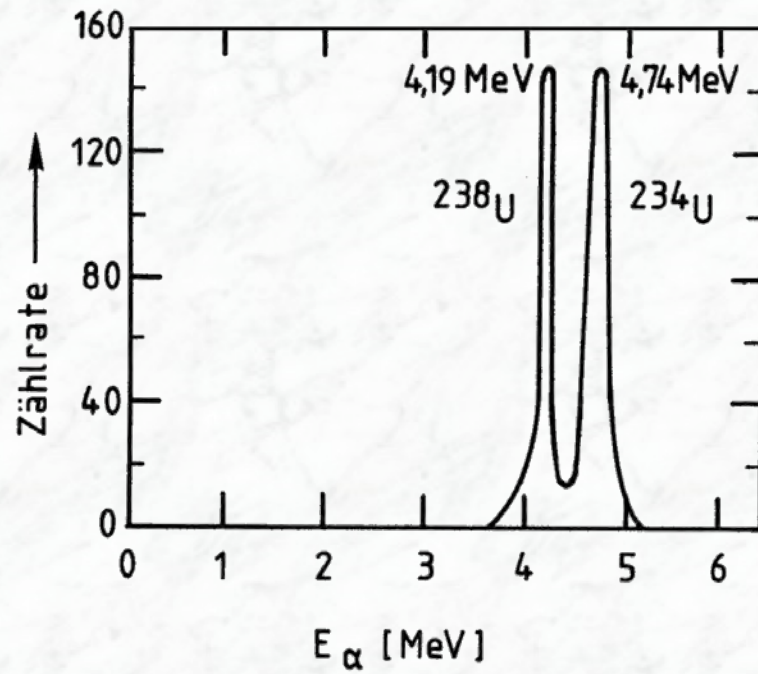


Principle of a cylindrical ionisation chamber  
[from Ref. 2]



Voltage pulse in a cylindrical proportional counter for different electronic time constants (shaping times [from Ref. 2])





Measured pulse height spectrum of  $\alpha$  particles of a  $^{234}\text{U} / ^{238}\text{U}$  mixture; [from Ref. 3]

Gas	Dichte $\rho[g/cm^3]$	$I_0[eV]$	$W[eV]$	$n_p[cm^{-1}]$	$n_T[cm^{-1}]$
$H_2$	$8.99 \cdot 10^{-5}$	15.4	37	5.2	9.2
$He$	$1.78 \cdot 10^{-4}$	24.6	41	5.9	7.8
$N_2$	$1.25 \cdot 10^{-3}$	15.5	35	10	56
$O_2$	$1.43 \cdot 10^{-3}$	12.2	31	22	73
$Ne$	$9.00 \cdot 10^{-4}$	21.6	36	12	39
$Ar$	$1.78 \cdot 10^{-3}$	15.8	26	29	94
$Kr$	$3.74 \cdot 10^{-3}$	14.0	24	22	192
$Xe$	$5.89 \cdot 10^{-3}$	12.1	22	44	307
$CO_2$	$1.98 \cdot 10^{-3}$	13.7	33	34	91
$CH_4$	$7.17 \cdot 10^{-4}$	13.1	28	16	53
$C_4H_{10}$	$2.67 \cdot 10^{-3}$	10.8	23	46	195

Tabelle 1.2: Zusammenstellung einiger Eigenschaften von Gasen. Angegeben sind der mittlere Energieverlust  $W$  pro erzeugtes Ionenpaar, das mittlere effektive Ionisationspotential pro Hüllenelektron  $I_0$ , die Anzahl der primär ( $n_p$ ) und insgesamt ( $n_T$ ) gebildeten Elektron-Ion-Paare pro  $cm$  bei Normaldruck für minimalionisierende Teilchen [94, 32, 104, 8].

[from Ref. 3]

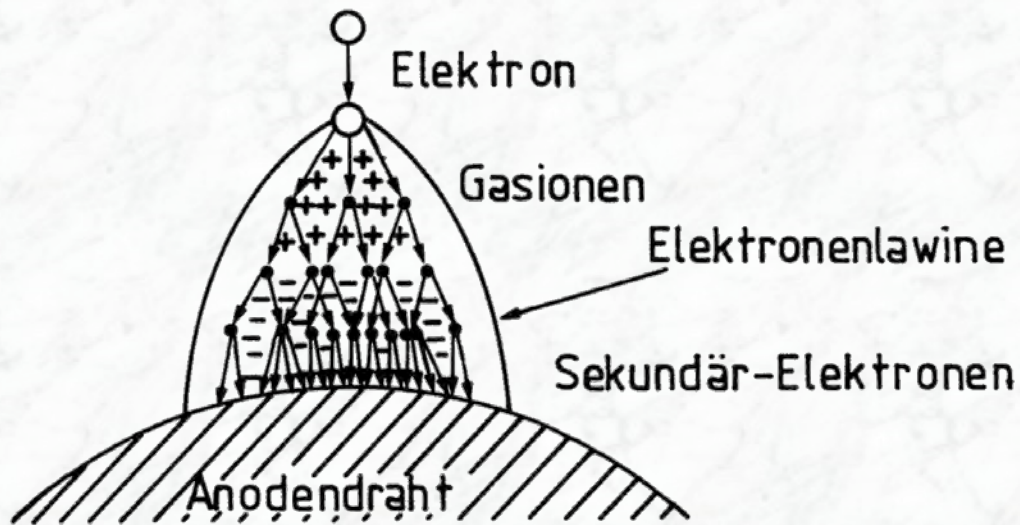
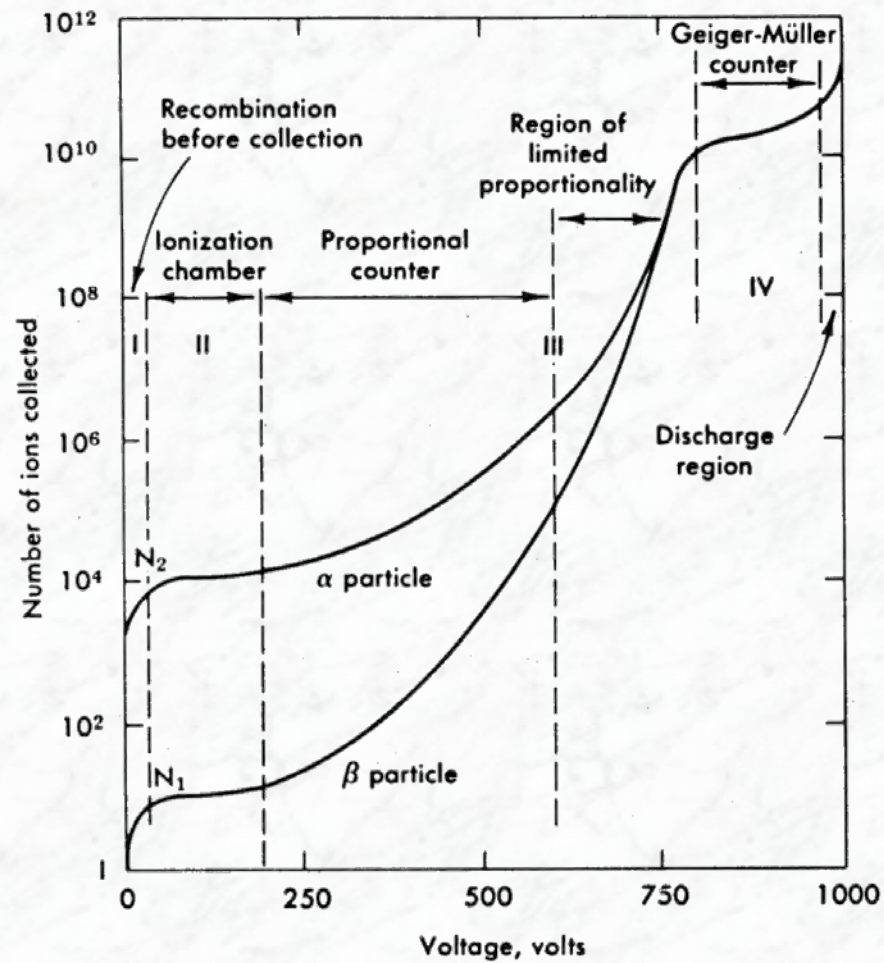


Illustration of avalanche charge multiplication in the vicinity of the anode wire in a proportional counter. Due to lateral diffusion, a drop-like avalanche develops. [from Ref. 3]





Number of collected charge carriers (ions) as a function of the applied voltage in a cylindrical gas-filled detector [from Ref. 2]



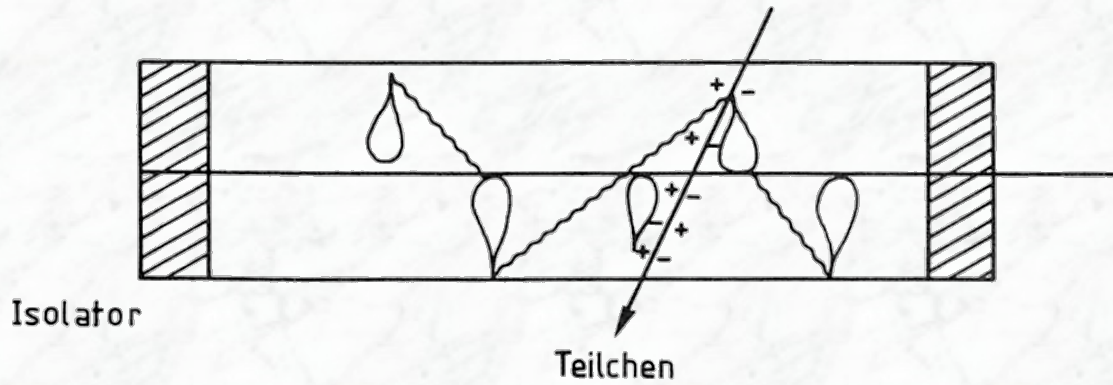
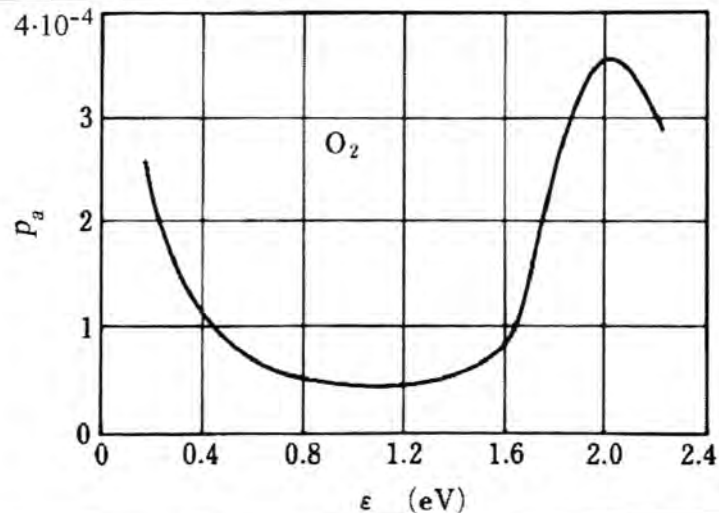


Illustration of the transverse avalanche propagation in a Geiger-Müller counter [from Ref. 3]

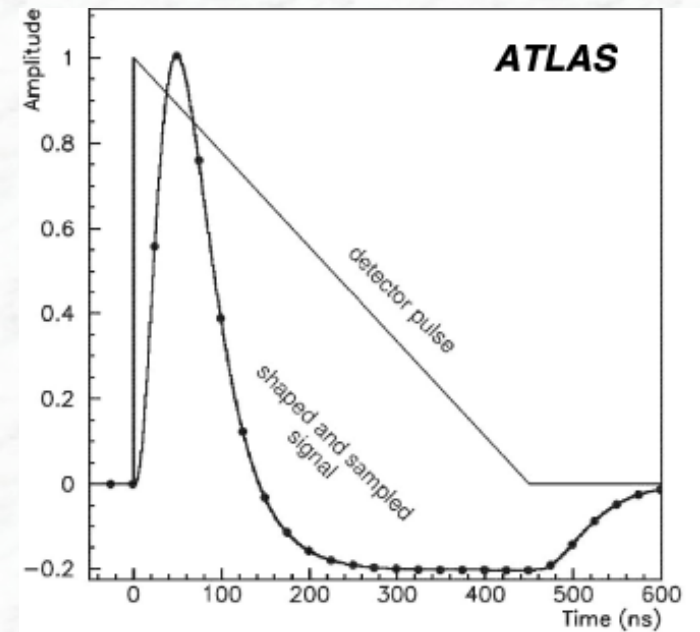
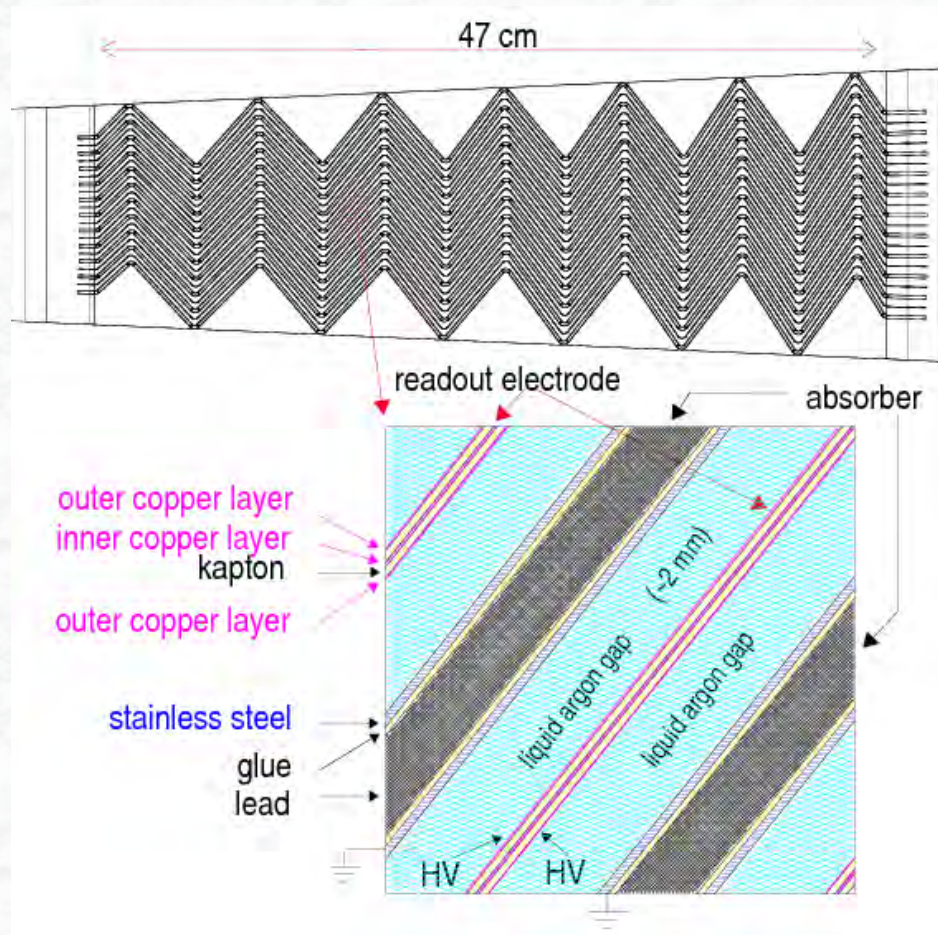
Gas	$p_a$	$n_s$ ( $s^{-1}$ )	$t_a$ (ns)
CO <sub>2</sub>	$6.2 \times 10^{-9}$	$2.2 \times 10^{11}$	$7.1 \times 10^5$
O <sub>2</sub>	$2.5 \times 10^{-5}$	$2.1 \times 10^{11}$	$1.9 \times 10^2$
H <sub>2</sub> O	$2.5 \times 10^{-5}$	$2.8 \times 10^{11}$	$1.4 \times 10^2$
Cl	$4.8 \times 10^{-4}$	$4.5 \times 10^{11}$	$5.0 \times 10^0$

Attachment probability for electrons  $p_a$ , number of collisions per second  $n_s$  and average time for attachment  $t_a$  without an electric field [from Ref. 1]



Attachment probability  $p_a$  for electrons in O<sub>2</sub> per collision as function of the electron energy  $\epsilon$  [from Ref. 3]

## Example: the liquid argon calorimeter of the ATLAS experiment



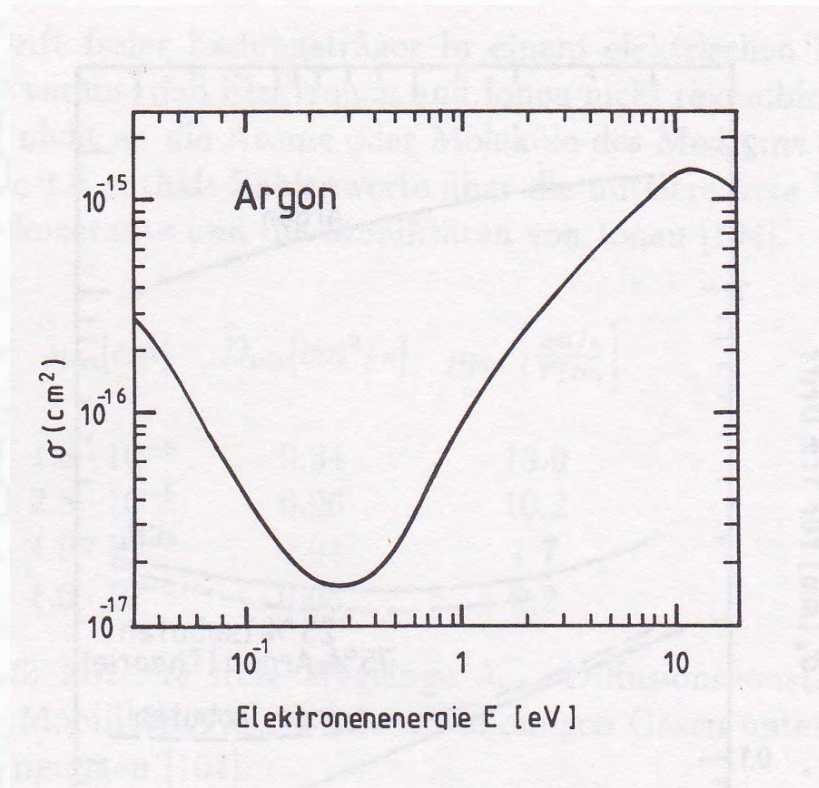
(the ATLAS liquid argon calorimeter uses current-sensitive amplifiers; measurement of the initial current!)



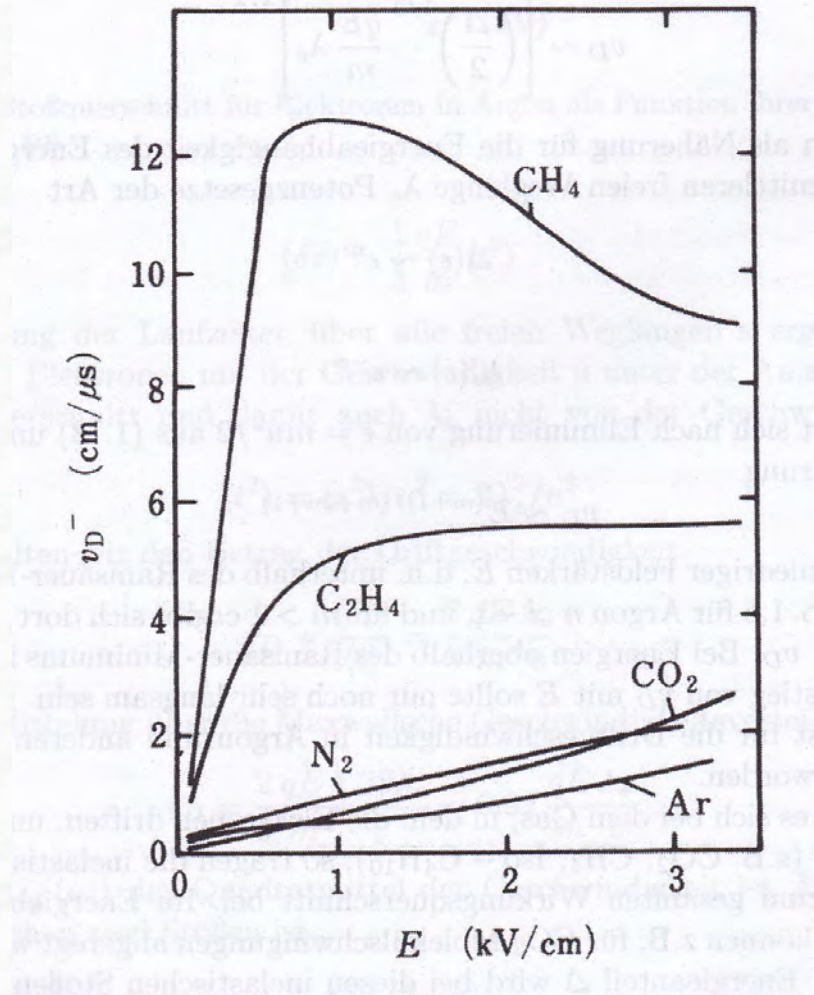
Gas	Massenzahl	$u$ (cm/s)	$D^+$ (cm <sup>2</sup> /s)	$\mu^+$ (cm <sup>2</sup> s <sup>-1</sup> V <sup>-1</sup> )	$\lambda$ (10 <sup>-5</sup> cm)
H <sub>2</sub>	2.02	$1.8 \times 10^5$	0.34	13.0	1.8
He	4.00	$1.3 \times 10^5$	0.26	10.2	2.8
Ar	39.95	$0.41 \times 10^5$	0.04	1.7	1.0
O <sub>2</sub>	32.00	$0.46 \times 10^5$	0.06	2.2	1.0
H <sub>2</sub> O	18.02	$0.61 \times 10^5$	0.02	0.7	1.0

Thermal velocities  $u$ , diffusion coefficients  $D^+$ , mobilities  $\mu^+$  and mean free path lengths  $\lambda$  for positive ions in different gases at normal pressure  $p_0$  [from Ref. 1].

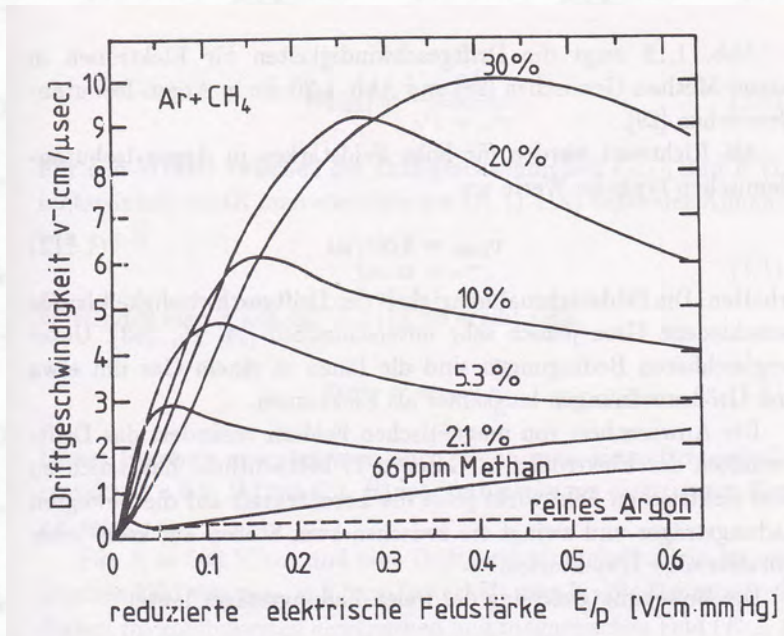
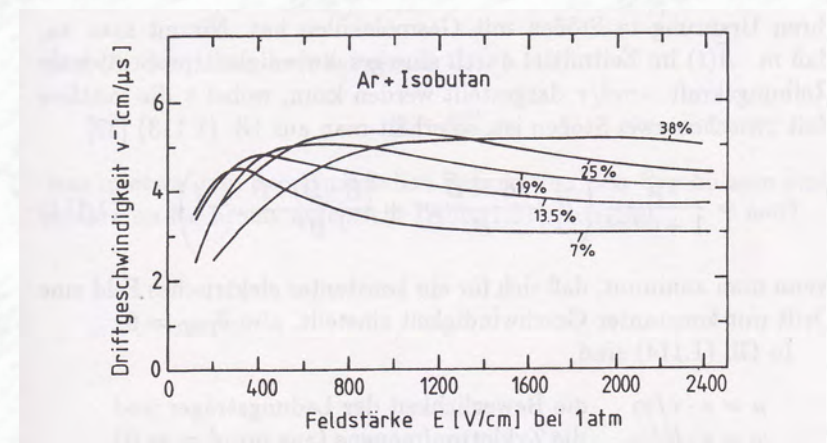
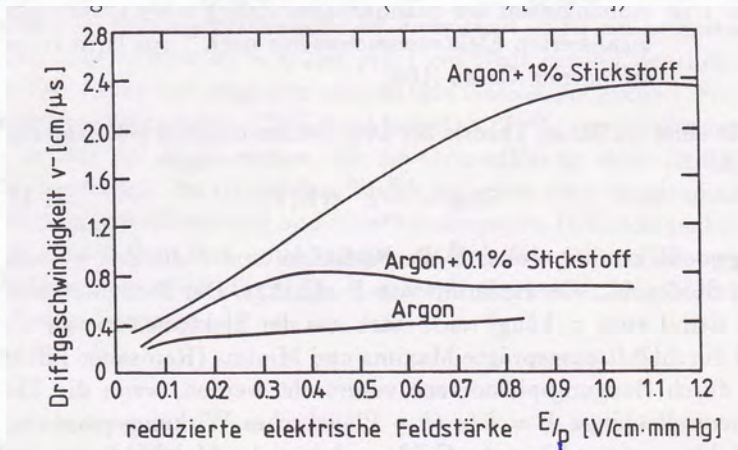




Scattering cross section  $\sigma$  for electrons in argon gas as a function of their kinetic energy [from Ref. 1].



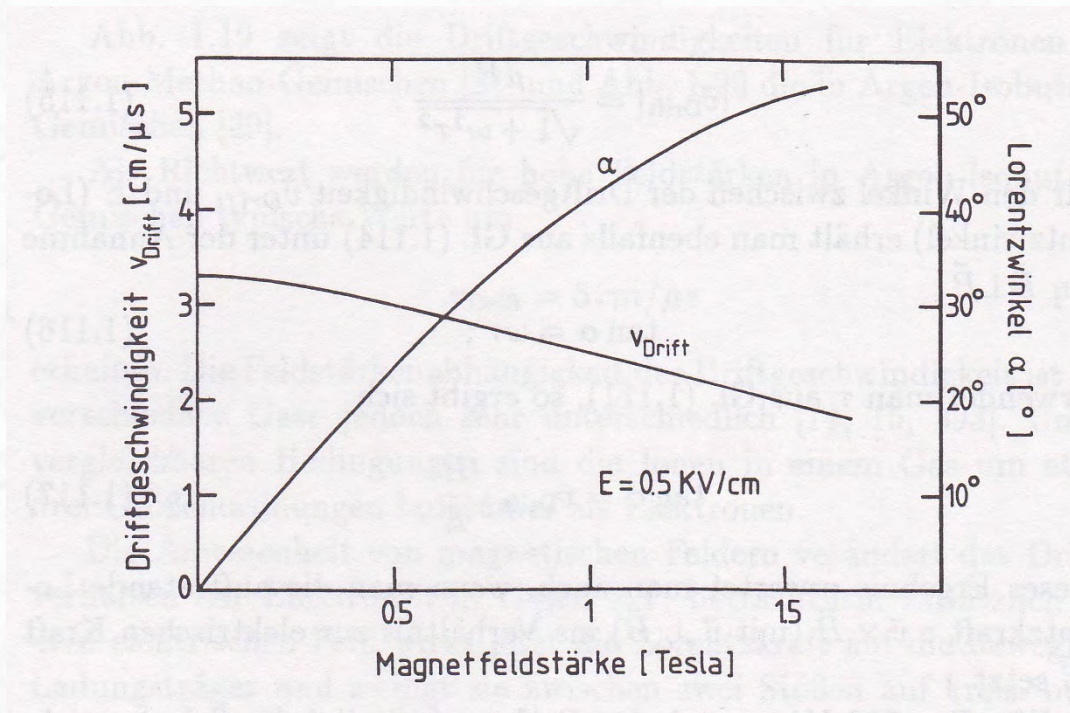
Drift velocity of electrons in various gases at normal pressure as a function of the electric field strength [from Ref. 1].



- The drift velocity in argon is relatively low, compared to other gases
- It can be significantly increased by the admixture of other gases, like (Ar, N<sub>2</sub>), (Ar, CO<sub>2</sub>), (Ar, CH<sub>4</sub>) or (Ar, C<sub>4</sub>H<sub>10</sub>)

Drift velocities of electrons in pure argon and in argon with admixtures of nitrogen, methane, and isobutane as a function of the reduced field strength ( $E/p$ ) or field strength ( $E$ ) [from Ref. 3].





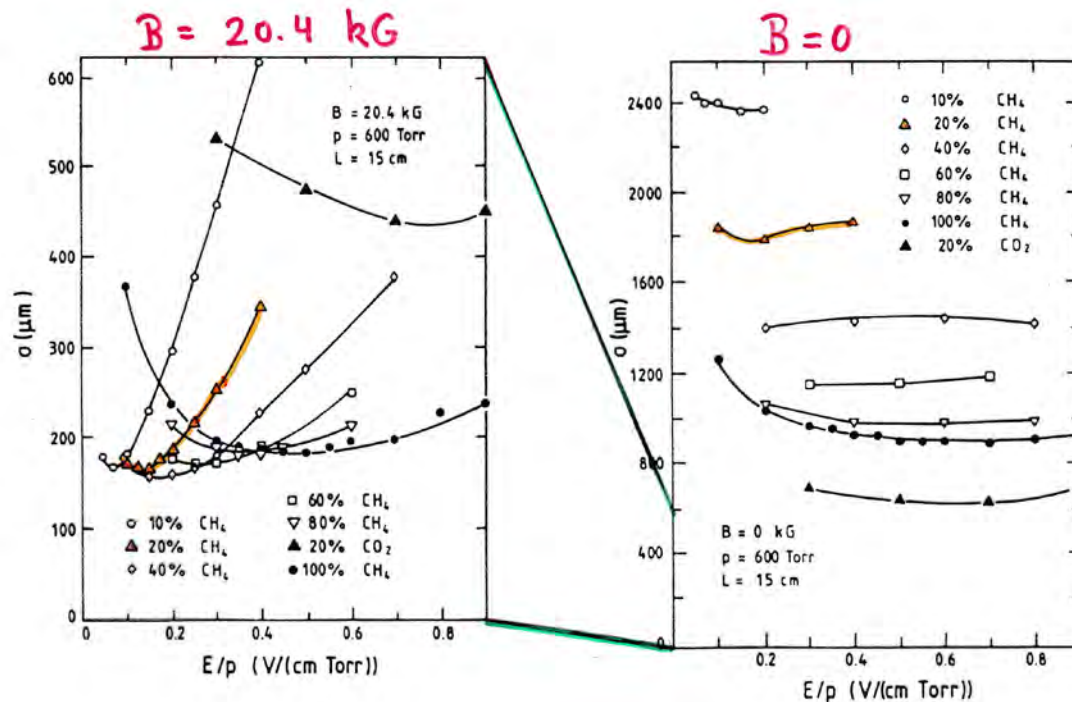
Drift velocities of electrons and Lorentz angle in a gas mixture of argon (67.2%), isobutane (30.3%) and methylal (2.5%) as a function of the magnetic field strength. The magnetic field is oriented perpendicular to the electric field [from Ref. 3].

Typical magnetic field strengths in particle physics experiments in the (inner detector volume, used for momentum determination)

LEP and Tevatron experiments: ~1.5 Tesla  
 ATLAS: 2.0 Tesla  
 CMS: 3.8 Tesla

→ sizeable effects

## Diffusion with and without a magnetic field:



Standard deviation of an originally point-like electron cloud transverse to the drift direction (E-field) due to diffusion after a drift distance of 15 cm without a magnetic field (right) and within a 2.04 T magnetic field parallel to the electric field (left), i.e. drift parallel to E [from Ref. 1].

→ significantly lower diffusion inside a magnetic field

important for position sensitive detectors (tracking detectors) like drift chambers and time projection chambers (→ Chapter 5)